JACS
JOURNAL OF THE AMERICAN CHEMICAL SOCIETY

Communication

pubs.acs.org/JACS

Photonic Crystal Kinase Biosensor

Kelsey I. MacConaghy, Christopher I. Geary, Joel L. Kaar,* and Mark P. Stoykovich*

Department of Chemical and Biological Engineering, University of Colorado, Boulder, Colorado 80309, United States

Supporting Information

ABSTRACT: We have developed a novel biosensor for kinases that is based on a kinase-responsive polymer hydrogel, which enables label-free screening of kinase activity via changes in optical properties. The hydrogel is specifically designed to swell reversibly upon phosphorylation of a target peptide, triggering a change in optical diffraction from a crystalline colloidal array of particles impregnated into the hydrogel. Diffraction measurements, and charge staining, confirmed the responsive nature of the hydrogel. Moreover, the change in diffraction of the hydrogel upon treatment with kinase exhibited a time- and dose-dependent response. A theoretical model for ionic polymer networks describes the observed optical response well and can be used to quantify the extent of phosphorylation.

Protein kinases are a critical family of enzymes that modulate virtually all cellular processes, including differentiation, proliferation, motility, and apoptosis, and thus cell function.[1,2] Modulation of cell function by kinases is the result of the phosphorylation of target protein substrates that are involved in intracellular signaling pathways. At the molecular level, the phosphorylation of protein substrates provides a mechanism by which target proteins may be activated or deactivated. The resulting activation or deactivation of target proteins can, in turn, lead to aberrant signal transduction if levels of kinase activity are altered, as is the case in many disease states. Due to their central role in signal transduction, kinases have been implicated in a myriad of diseases, making kinases among the most important targets for therapeutic molecules.[3]

Despite the importance of kinases as potential drug targets, robust, high-throughput screening methods for kinase inhibitors and activators are sorely lacking. Kinases are inherently difficult to assay due to the lack of measurable signal (i.e., pH or color change) upon protein phosphorylation. Conventional biochemical methods to assay kinase activity nearly all use radiolabeled or fluorescent substrates or phospho-specific antibodies.[4−6] Such methods, while sensitive, require expensive reagents and frequently involve multiple steps. Notably, phospho-specific antibodies are also challenging to generate and of limited availability for phosphoserine and -threonine residues.[7] Additionally, fluorescent methods, which are widely based on quenching, polarization, or resonance energy transfer, are prone to signal interference by small molecules that may fluoresce or quench fluorescent signals. Kinase screening efforts may alternatively rely on biophysical binding techniques such as NMR,[8] surface plasmon resonance,[9] differential scanning fluorimetry (i.e., thermal shift assay),[10] and quartz crystal microbalance,[11] although traditional binding assays are limited in their ability to measure changes in catalytic activity. More recently, screening methods based on improved mass spectroscopy techniques,[12] computational approaches,[13,14] and label-free nanoparticle aggregation assays[15−18] have been reported. Ultimately, the development of high-throughput kinase screening platforms would greatly facilitate the discovery of potential drug candidates as well as probes for studying cellular mechanisms involved in disease and, moreover, kinase profiling.

Here, we present a novel photonic crystal biosensor for the optical detection of peptide phosphorylation and, thus, kinase activity. The biosensor is composed of a crystalline colloidal array (CCA) polymerized into a hydrogel matrix. The photonic crystal, shown in Scheme 1, consists of negatively charged, vinyl-functionalized polystyrene particles that self-assemble into a pseudocrystal structure that diffracts light in the visible spectrum. Once polymerized, the hydrogel is functionalized with a kinase recognition sequence that is subject to phosphorylation, which alters the electrostatic environment within the hydrogel. The resulting change in the electrostatics induces a Donnan potential that causes the hydrogel to swell and, in turn, the lattice spacing of the CCA to increase and the wavelength of peak diffraction to red shift. Such an optical response can be monitored spectrophotometrically, after rinsing of mobile ions, to readily quantify the effect of kinase inhibitors and activators on phosphorylation activity. Incorporation of photonic crystals into swellable polymer networks has been reported previously for detecting pH changes and charged species, including small molecules and metal ions.[19−22] Importantly for biosensing applications, because the CCAs developed here diffract light at visible wavelengths (≥400 nm), the adsorption of light by small molecules, which typically adsorb light in the UV range, will not

Scheme 1. Fabrication of a Kinase Responsive CCA Biosensor

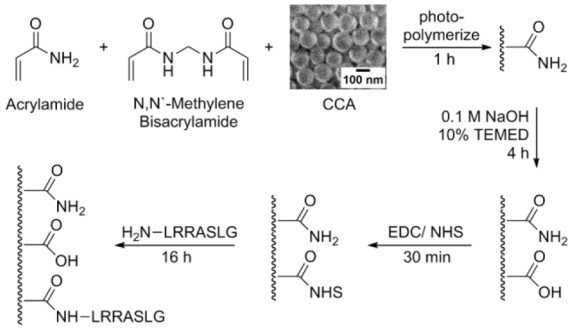

Received: March 27, 2014
Published: April 24, 2014

   dx.doi.org/10.1021/ja5031062 | J. Am. Chem. Soc. 2014, 136, 6896−6899

interfere with the CCA signal. Additionally, because the sensing platform is reagentless, kinase activity may be screened without exogenous labels or components, representing a significant advantage over conventional kinase assay methods.

Optically diffracting hydrogel thin films (126.4 ± 0.7 μm thick) were fabricated on vinyl-functionalized plastic substrates via the process outlined in Scheme 1. Specifically, acrylamide was photopolymerized in the presence of a colloidal suspension of charged, vinyl-functionalized polystyrene (PS) latex spheres (10−12% w/w), resulting in the cross-linking of a stable CCA within the hydrogel network. The negatively charged polystyrene particles were synthesized by emulsion polymerization in water using surfactants to stabilize the initial micelle formation and the polymer particles that were formed.[23,24] Dynamic light scattering (Figure S1 in the Supporting Information (SI)) and scanning electron microscopy were used to characterize the resulting spheres, which were found to pack into a dense array in thin films (see the scanning electron micrograph in Scheme 1) as well as to be monodisperse in size with a diameter of 110 ± 2 nm. In solution, the formation of the CCA is the result of the electrostatic forces between negatively charged sulfonate groups (zeta potential of −33 ± −2 mV) on the surface of the polystyrene particles. Electrostatic repulsion between the particles causes them to adopt a face-centered cubic lattice structure that has the lowest configurational energy. The crystal structure and thus volume of the hydrogel dictates the diffraction spectrum of the CCA sensor through Bragg's law.[25] Figure 1

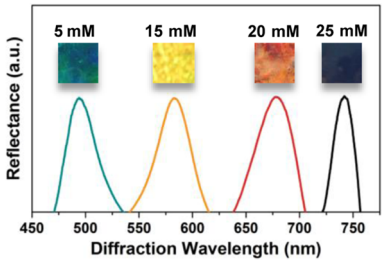

Figure 1. Red shift in peak optical reflectance of hydrogel-encapsulated CCAs with increasing concentration of immobilized negatively charged groups (at pH 5.5). The inset images (~5 × 5 mm^2) show visual color changes of the hydrogels. The total concentrations of negative charge from 5 to 25 mM, as indicated above each image, were measured by colorimetric staining.

shows example diffraction spectra of hydrogel-encapsulated CCAs as a function of immobilized carboxylate groups, the concentration of which was controlled by varying the hydrolysis time. Reflectance spectroscopy is used to quantify the wavelength of peak diffraction, although distinct changes in film color can also be observed by eye. The photograph corresponding to a total negative-charge concentration of 25 mM appears almost black due to excessive swelling of the hydrogel, which causes the hydrogel to diffract at wavelengths beyond the visible spectrum.

Upon preparation of the CCA-containing hydrogel, the hydrogel was functionalized with a peptide substrate (LRRASLG) for protein kinase A (PKA). The target LRRASLG peptide contains two positively charged arginine residues and has a net positive charge of +0.5 at neutral pH after phosphorylation of the serine. Full experimental details, including peptide conjugation, may be found in the SI. Briefly, peptide functionalization was enabled by converting free amide groups in the hydrogel to carboxylate groups through base hydrolysis. A two-step EDC/NHS reaction was subsequently used to form an amide linkage between the carboxylates in the hydrogel and the N-terminus amine of the peptide substrate. The functionalization reaction was performed in a high ionic strength environment to shield the immobilized negative charges, thus preventing excessive swelling and mechanical failure (i.e., delamination, fracturing, or wrinkling) of the hydrogel. Each step of the fabrication process was confirmed by diffraction measurements and the extent of reaction was quantified by staining for immobilized charges. Prior to measuring optical diffraction, the hydrogels were rinsed extensively to remove free, mobile ions, which would interfere with the sensor's response. By rinsing the sensor, the structure and response of the CCA is dependent only on the immobilized charges. To stain the hydrogels for negative and positive charges, the gel was reacted with toluidine blue O and acid orange 7, respectively, as reported previously.[26,27] The hydrogels were incubated in aqueous solutions containing each stain for 3 h to allow for complete dye adsorption, after which the hydrogels were rinsed to remove any loosely adsorbed dye. Following rinsing, the bound dye was extracted via treatment with a strong acid or base and quantified by UV−vis absorbance. For determination of immobilized charge concentrations in the hydrogel, the ratio of dye to immobilized charge was assumed to be 1:1.

The immobilized charge concentration in the hydrogel-encapsulated CCAs is shown in Figure 2, as quantified by charge

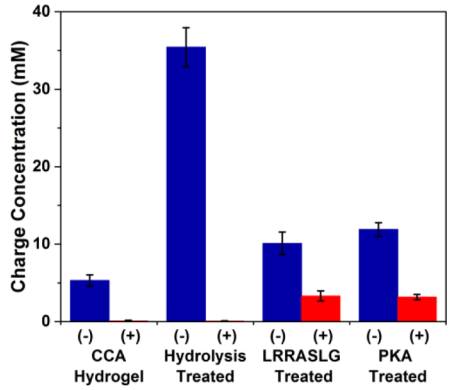

Figure 2. Concentration of immobilized charge in the kinase responsive CCA-containing hydrogels characterized by colorimetric staining. The blue and red bars represent negative (−) and positive (+) charge concentrations, respectively. The positive charge concentration in the CCA-containing hydrogel and the hydrolyzed hydrogel were determined to be negligible within error. Error bars represent ±1σ, as measured for the first three steps for 30 samples. The PKA treatment was performed at a concentration of 16 U/μL and 8 h and is reported for 3 independent samples.

staining, following the polymerization, hydrolysis, and peptide functionalization steps. Charge concentration was determined on a per unit volume basis of the unswollen hydrogel. The hydrogels had an initial wavelength of peak diffraction of 500 nm and a concentration of negative charge of 5 mM, which was due to the presence of the PS spheres. Hydrolysis increased the amount of negative charge immobilized in the hydrogel by 7-fold, although this represents a low overall conversion (<1 mol %) of the available amide groups to carboxylates. The larger concentration of immobilized charge increases the Donnan potential, causing the hydrogel to swell and the wavelength of peak diffraction to red shift to >800 nm. Functionalizing the hydrogel with LRRASLG reduced the concentration of negative charges, due to reactive coupling through the carboxylate groups,

dx.doi.org/10.1021/ja5031062 | J. Am. Chem. Soc. 2014, 136, 6896−6899

and increased the concentration of positive charges due to the two arginine residues (with pK_a's of 12.48) present in the peptide. Based on the charge concentration and an overall mole balance, the concentration of peptide immobilized in the hydrogel was calculated to be ~10 mM. The reduction in negative charge was more significant than that expected based on the corresponding increase in the concentration of positive charge. Peptide functionalization also caused a dramatic blue shift in the optical response to a wavelength of peak diffraction of 495 nm, which was less than that of the initial CCA. Likely these observed effects were due to the formation of ionic cross-links between positive and negative charges in the hydrogel, which reduced the concentrations of free charges and increased gel stiffness, resulting in less swelling. Potential cross-linking of immobilized charges was accounted for in the estimation of immobilized peptide concentration. In comparison, unhydrolyzed samples and samples without peptide showed no change in charge concentration.

The screening and quantification of kinase activity using the photonic crystal biosensor was demonstrated as a function of phosphorylation reaction time and enzyme concentration. Time course measurements (Figure 3a) were performed by incubating

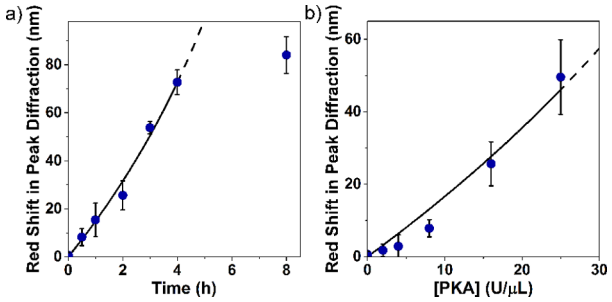

Figure 3. Red shift in the wavelength of peak diffraction as a function of (a) time upon treatment with 16 U/μL of PKA and (b) PKA concentration for 2 h treatments. The solid black curves represent model predictions over the range fitted, and the dashed curves are extrapolations from the model. Error bars represent $\pm 1\sigma$ from the mean for 3 independent samples.

the biosensor at 30 °C in 0.5 mL of reaction buffer (50 mM Tris-HCl, pH 7.5, with 10 mM $MgCl_2$ and 1 mM ATP) with 16 U/μL of PKA. The reaction was quenched by heating the biosensor at 65 °C for 20 min to denature the enzyme. The biosensor was then thoroughly rinsed in water to remove any excess reactants or mobile ions that may reduce the extent of swelling. The red shift in the wavelength of peak diffraction is reported, representing the difference in Bragg diffraction between post- and pre-PKA treatment (see Figure S3 for raw spectra). The red shift in the wavelength of peak diffraction due to the increase in immobilized negative charge was detected in as short as 30 min and increased with reaction times from 0 to 4 h, whereas after 4 h a plateau in sensor response was observed. Control samples prepared with phosphorylated LRRASLG (LRRApSLG) indicated that a red shift in peak diffraction of 100 nm corresponded to 30% phosphorylation (Figure S2). Based on this, the response of the sensor in the time course plot is presumably limited by the extent of phosphorylation of the immobilized peptide. Limitations in phosphorylation may result from the loss of PKA activity from enzyme instability as well as partial inaccessibility of the immobilized peptide. Inamori et al.[28] previously observed that phosphorylation of LRRASLG tethered to gold surfaces by PKA was limited to ~20 mol % of that in solution. Moreover, while it is also plausible that this plateau may result from diffusional limitations, this is unlikely based on previous literature that has shown that proteins of similar size were able to diffuse 50 μm into CCA-impregnated hydrogels within 20 min, which is much deeper than the optically active region of the film being probed here.[29,30] Additionally, a dose response curve, showing red shift in peak diffraction as a function of PKA concentration, is shown in Figure 3b. Phosphorylation of the peptide by PKA can also be detected by staining as a small increase in the immobilized negative charge concentration (Figure 2, PKA treated samples). However, this response is significantly weaker than that measured optically, indicating the higher sensitivity of the CCA's optical response as compared to that of the charge staining assay. Control samples (not shown) for both the time course and dose response data were incubated in the presence of PKA, but without ATP. Time course controls were incubated for 8 h (also with 16 U/μL enzyme), and dose response controls were incubated with 25 U/μL enzyme (also for 2 h). Both sets of controls showed a shift in the wavelength of peak diffraction of <1 nm upon enzyme treatment, confirming that the apparent response was due solely to phosphorylation. Moreover, the sensor showed no change in response in the presence of exogenous charged molecules, indicating that there is no interference from such molecules (Figure S4).

To demonstrate the utility of the CCA sensor to screen for kinase inhibitors, the sensor response to PKA activity in the presence of the small molecule kinase inhibitor H-89 was measured (Figure 4). The small molecule inhibitor H-89

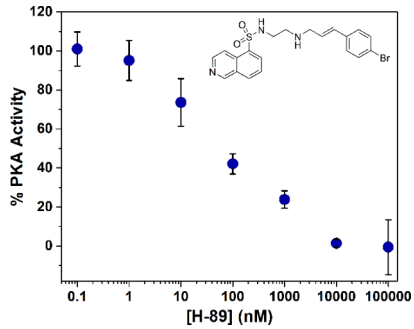

Figure 4. Sensitivity of kinase responsive CCA sensor to PKA inhibition by H-89 (inset structure). Inhibition of PKA by H-89 was measured with varying inhibitor concentrations (0–10^5 nM) and 16 U/μL of PKA. Hydrogel-encapsulated CCAs were incubated with the enzyme and inhibitor for 3 h at 30 °C. Error bars represent $\pm 1\sigma$ from the mean for 3 independent samples.

competitively inhibits PKA by binding to the ATP binding cleft.[31] The activity of PKA in the presence of H-89 was measured by preincubating 16 U/μL of PKA with 0.1 nM–100 μM H-89 for 10 min in reaction buffer (50 mM Tris-HCl, pH 7.5, 10 mM $MgCl_2$, 100 μM ATP). Following incubation of PKA with H-89, the CCA sensor was immersed in the reaction solution for 3 h at 30 °C after which residual PKA activity was quenched as above and the system was rinsed with water. As expected, increasing the concentration of H-89 decreased the red shift in peak diffraction, which is attributed to decreasing PKA activity. Notably, the IC50 value of H-89 was determined to be 68 nM, which is in agreement with previously reported literature values.[31]

The optical response of CCAs encapsulated in the kinase responsive hydrogel is dependent on not only the kinase activity

dx.doi.org/10.1021/ja5031062 | J. Am. Chem. Soc. 2014, 136, 6896–6899

but also (i) the material properties of the hydrogel, (ii) the immobilized charge distribution in the hydrogel, and (iii) the ionic character of the surrounding environment. A model of swelling in ionic polymer networks elucidates these dependencies and was used to fit the time course and dose response data in Figure 3 (solid curves; see SI for full model details). The model predictions fit the experimental data well and allow for quantification of the extent of phosphorylation and enzyme kinetics including k_{cat} from the optical response (Figure S5). Deviation of the time course data from the model predictions at long incubation times (8 h) may be, as suggested previously, due in part to the loss in PKA activity over time or peptide inaccessibility. By elucidating the critical parameters that are associated with the diffraction of the biosensor in response to kinase activity, the model ultimately may be used to improve the sensitivity of the sensor and thus reduce the detection limit and permit shorter reaction times. For example, the model predicts that increased sensitivity may be achieved by increasing the concentration of accessible peptide, eliminating extraneous charges immobilized in the hydrogel (e.g., unreacted carboxylate functionalities), or by lowering the elastic restoring force upon swelling by reducing Young's modulus of the gel (i.e., cross-linking density). Excess negative charges in the polymer backbone may be eliminated by linking the peptide through chemistries that do not require hydrolysis of the hydrogel (e.g., click reactions). Furthermore, although diffusional limitations do not affect the response of the sensor toward PKA, such limitations, which impact sensor response, with larger enzymes or proteins may be reduced by altering cross-linking density.

In summary, novel photonic crystal-containing polymer hydrogels that are responsive to peptide phosphorylation were developed for assaying kinase activity. Such hydrogels may be used as a sensing platform to identify kinase inhibitors or activators of kinase pathways, as well as for assaying kinase selectivity. The lack of exogenous fluorescent reagents or labels, furthermore, enhances the potential utility of the hydrogels for high-throughput screening, which may be enabled through preparation of the hydrogels in a multiplex format. Though the photonic crystal biosensor was specifically developed for screening purified kinases, washing and detection in pure water will allow for assaying biologically complex samples as well. We have also demonstrated that the sensor can be used to detect the reverse (i.e., dephosphorylation) reaction, involving the removal of immobilized negative charges, by phosphatases (Figure S6). More broadly, such hydrogels may be used to assay the activity of other enzymes that catalyze post-translational modifications that alter substrate charge (e.g., sulfonation, acetylation, carboxylation, or amidation), thus providing a platform to screen a broad spectrum of protein or biomolecule modifications.

■ ASSOCIATED CONTENT

Supporting Information

Detailed materials and methods, theoretical model of biosensor response, and additional detection results. This material is available free of charge via the Internet at http://pubs.acs.org.

■ AUTHOR INFORMATION

Corresponding Authors

joel.kaar@colorado.edu
mark.stoykovich@colorado.edu

Notes

The authors declare no competing financial interest.

■ ACKNOWLEDGMENTS

Support was provided by the Univ. of Colorado Liquid Crystal Material Research Center (NSF DMR0820579) and NIH Pharmaceutical Biotechnology Training Program (NIH 5T32GM8732).

■ REFERENCES

(1) Hunter, T. *Cell* **2000**, *100* (1), 113.
(2) Miduturu, C. V.; Deng, X. M.; Kwiatkowski, N.; Yang, W. N. A.; Brault, L.; Filippakopoulos, P.; Chung, E.; Yang, Q. K.; Schwaller, J.; Knapp, S.; King, R. W.; Lee, J. D.; Herrgard, S.; Zarrinkar, P.; Gray, N. S. *Chem. Biol.* **2011**, *18* (7), 868.
(3) Cohen, P.; Alessi, D. R. *ACS Chem. Biol.* **2013**, *8* (1), 96.
(4) Ko, K. C.; Choi, M. H.; Rho, J. K.; Park, S. H. *Sens. Actuators B* **2013**, *178*, 434.
(5) Prevel, C.; Pellerano, M.; Van, T. N.; Morris, M. C. *Biotechnol. J.* **2013**, *9* (2), 253.
(6) Jeong, H. J.; Ohmuro-Matsuyama, Y.; Ohashi, H.; Ohsawa, F.; Tatsu, Y.; Inagaki, M.; Ueda, H. *Biosens. Bioelectron.* **2013**, *40* (1), 17.
(7) Koerber, J. T.; Thomsen, N. D.; Hannigan, B. T.; Degrado, W. F.; Wells, J. A. *Nat. Biotechnol.* **2013**, *31* (10), 916.
(8) Masterson, L. R.; Shi, L.; Metcalfe, E.; Gao, J. L.; Taylor, S. S.; Veglia, G. *Proc. Natl. Acad. Sci. U.S.A.* **2011**, *108* (17), 6969.
(9) Takeda, H.; Goshima, N.; Nomura, N. *Surface Plasmon Resonance: Methods and Protocols* **2010**, *627*, 131.
(10) Fedorov, O.; Niesen, F. H.; Knapp, S. *Kinase Inhibitors: Methods and Protocols* **2012**, *795*, 109.
(11) Xu, X.; Zhou, J.; Liu, X.; Nie, Z.; Qing, M.; Guo, M.; Yao, S. *Anal. Chem.* **2012**, *84* (11), 4746.
(12) Zinn, N.; Hopf, C.; Drewes, G.; Bantscheff, M. *Methods* **2012**, *57* (4), 430.
(13) Metz, J. T.; Johnson, E. F.; Soni, N. B.; Merta, P. J.; Kifle, L.; Hajduk, P. J. *Nat. Chem. Biol.* **2011**, *7* (4), 200.
(14) Shen, M. Y.; Zhou, S. Y.; Li, Y. Y.; Pan, P. C.; Zhang, L. L.; Hou, T. J. *Mol. Biosyst.* **2013**, *9* (3), 361.
(15) Oishi, J.; Asami, Y.; Mori, T.; Kang, J.-H.; Tanabe, M.; Niidome, T.; Katayama, Y. *ChemBioChem* **2007**, *8* (8), 875.
(16) Kang, J. H.; Asami, Y.; Murata, M.; Kitazaki, H.; Sadanaga, N.; Tokunaga, E.; Shiotani, S.; Okada, S.; Maehara, Y.; Niidome, T.; Hashizume, M.; Mori, T.; Katayama, Y. *Biosens. Bioelectron.* **2010**, *25* (8), 1869.
(17) Asami, Y.; Oishi, J.; Kitazaki, H.; Kamimoto, J.; Kang, J. H.; Niidome, T.; Mori, T.; Katayama, Y. *Anal. Biochem.* **2011**, *418* (1), 44.
(18) Xu, X.; Liu, X.; Nie, Z.; Pan, Y.; Guo, M.; Yao, S. *Anal. Chem.* **2011**, *83*, 52.
(19) Arunbabu, D.; Sannigrahi, A.; Jana, T. *Soft Matter* **2011**, *7* (6), 2592.
(20) Holtz, J. H.; Asher, S. A. *Nature* **1997**, *389* (6653), 829.
(21) Walker, J. P.; Asher, S. A. *Anal. Chem.* **2005**, *77* (6), 1596.
(22) Sharma, A. C.; Jana, T.; Kesavamoorthy, R.; Shi, L. J.; Virji, M. A.; Finegold, D. N.; Asher, S. A. *J. Am. Chem. Soc.* **2004**, *126* (9), 2971.
(23) Arunbabu, D.; Sannigrahi, A.; Jana, T. *J. Appl. Polym. Sci.* **2008**, *108* (4), 2718.
(24) Reese, C. E.; Guerrero, C. D.; Weissman, J. M.; Lee, K.; Asher, S. A. *J. Colloid Interface Sci.* **2000**, *232* (1), 76−80.
(25) Asher, S. A.; Holtz, J.; Liu, L.; Wu, Z. J. *J. Am. Chem. Soc.* **1994**, *116* (11), 4997.
(26) Nakajima, N.; Ikada, Y. *Bioconjugate Chem.* **1995**, *6* (1), 123.
(27) Uchida, E.; Uyama, Y.; Ikada, Y. *Langmuir* **1993**, *9* (4), 1121.
(28) Inamori, K.; Kyo, M.; Matsukawa, K.; Inoue, Y.; Sonoda, T.; Tatematsu, K.; Tanizawa, K.; Mori, T.; Katayama, Y. *Anal. Chem.* **2008**, *80* (3), 643.
(29) Baca, J. T.; Finegold, D. N.; Asher, S. A. *Analyst* **2008**, *133* (3), 385.
(30) Tong, J.; Anderson, J. L. *Biophys. J.* **1996**, *70* (3), 1505.
(31) Lochner, A.; Moolman, J. A. *Cardiovasc. Drug Rev.* **2006**, *24* (3−4), 261.